WIDE BANDWIDTH PIEZOELECTRIC MICRO ENERGY HARVESTER BASED ON NONLINEAR RESONANCE

Arman Hajati[1], Ruize Xu[2*], Sang-Gook Kim[2]
[1]FUJIFILM Dimatix, Santa Clara, CA, USA
[2]Massachusetts Institute of Technology (MIT), Cambridge, MA, USA
*Presenting Author: rzxu@mit.edu

Abstract: A new piezoelectric energy harvester is developed based on a doubly-clamped MEMS-scale non-linear resonator, which overcomes the limitations of conventional linear resonance beam-based piezoelectric energy harvesters in terms of power bandwidth and power density. The electromechanical tests show up to 1.5V (peak-to-peak) open circuit output voltage in a wide range of frequencies, which can be interpreted to have more than one order of magnitude improvements in comparison to the devices previously reported in both bandwidth (>20% of the peak frequency) and power density (up to 2W/cm^3 with an SSHI interface) at 1.3kHz. In this paper, design, modeling, fabrication, and testing of a wide bandwidth piezoelectric micro energy harvester are presented.

Keywords: energy harvesting, piezoelectric, wide-bandwidth

INTRODUCTION

A compact and low cost micro-energy generator, which perpetually harvests energy from ambient vibrations can be an ultimate solution for self-powered embedded sensors and smart systems. Additionally, the advancement of microelectronics technology has enabled the ultra-low power chips and systems, which can be operated with 10's of microwatts. It now becomes realistic and reasonable to employ MEMS-scale energy harvesters to power a wide range of wireless devices if they can harvest more than 10's of microwatts continuously over a wide range of uncertain environmental vibrations. Many groups have designed and developed a series of MEMS-scale piezoelectric energy harvesters based on linear cantilever resonating beams, which prevents deployment of them to real applications due to the inherent "Gain-Bandwidth Dilemma" [1]. In order to circumvent the "Gain-Bandwidth Dilemma," we recently developed and reported a non-linear resonant beam energy harvester, which utilizes the stretching strain in thin, doubly-clamped beams instead of the bending strain in cantilever structures [2, 3].

THEORETICAL ANALYSIS

Nonlinear Resonator Design and Modeling

Most piezoelectric energy harvesters have been designed based on a linear resonator, which is typically a cantilever with a proof mass. The output power of an energy harvester based on a linear resonator is proportional to the gain (Quality factor) of the resonator, which is inversely proportional to the bandwidth. Accordingly, there is a trade-off between the output power and the bandwidth. Since we cannot control the frequency of ambient vibrations, an energy harvester with a narrow bandwidth is impractical in real applications.

To overcome the limitation, a new design based on a nonlinear resonator is proposed [2]. Instead of a cantilever, the new design is based on doubly-clamped beams with two fixed ends and a proof mass in the middle (Fig. 1(a)). At large deflections (> thickness of the beam), the load-deflection relationship of the beam requires net stretching of the beam. By using variational methods [4], an approximate expression describing the large-amplitude load-deflection behavior is:

$$F = \left(\frac{\pi^4}{6}\right)\left[\frac{EWH^3}{L^3}\right]x + \left(\frac{\pi^4}{8}\right)\left[\frac{EWH}{L^3}\right]x^3 \qquad (1)$$

where F is the load, E is Young's modulus, W, H and L are the width, thickness and length of the beam respectively, and x is the deflection. It should be noted that the applied load F is not linearly dependent on deflection x. Moreover, the solution has two parts; the first term results from the small-amplitude bending, while the second nonlinear term comes from stretching. The nonlinear term implies that the stiffness of the beam increases as the deflection increases, and becomes the amplitude-stiffened Duffing spring [5].

To model and analyze the doubly-clamped beam-based nonlinear resonator, it is assumed that the base is fixed and a sinusoidal force is applied to the proof mass. Then a mechanical lumped model (Fig. 1(b)) and electrical lumped models (Fig. 1(c), (d)) are constructed, which consist of a proof mass, a linear spring due to bending, a nonlinear spring due to stretching, a mechanical damper and an electrical damper. The dynamic equation of the mass-spring-damper system is,

$$m\ddot{x} + b\dot{x} + k_L x + k_N x^3 = F\cos(\omega t) \qquad (2)$$

where m is the proof mass, b is the total damping including structural damping, aerodynamic damping and electrical damping, k_L is the linear stiffness, k_N is the nonlinear stiffness, ω is the excitation frequency, and t is time.

Substituting linear and nonlinear stiffness's and

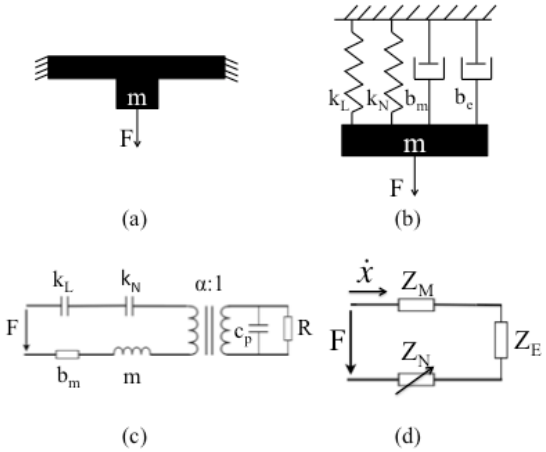

Figure 1. Lumped models of nonlinear resonator based energy harvester. (a) Simplified dynamic model. (b) Mechanical lumped model. (c) Electrical lumped model. (d) Electrical lumped model with impedances.

damping coefficients into Eq. (2) and solving for the deflection, a cubic equation can be obtained:

$$\frac{9k_N^2}{16}\left(1+\frac{b_s^2}{k_L^2}\omega^2\right)x^6+\frac{3k_N}{2}\left[k_N+\frac{(b_a+b_e+b_s)b_s}{k_L}\omega^2-m\omega^2\right]x^4 +\left[(b_a+b_e+b_s)^2\omega^2+(k_L-m\omega^2)^2\right]x^2-m^2a^2=0 \tag{3}$$

where b_s, b_a, b_e are structural damping, aerodynamic damping and electrical damping respectively, and a is the excitation acceleration. The multiple solutions of Eq. (3) are illustrated in Fig. 2. The tilted peak resulting from the nonlinearity of *Duffing* mode resonance indicates a wider bandwidth, if the resonator can stay on the upper envelope (high-energy) of this curve. Depending on the initial conditions, a system may work at different regions denoting by different colors in Fig. 2. If sweeping frequency from low to high, the system will work in the unique solution region first at small deflection, then the deflection will increase along the high-energy stable region, until it jumps down to low energy stable region. If sweeping the frequency high to low, the response will go along the low-energy stable region until it jumps up to high-energy stable region again. The jump-down and jump-up frequencies are marked by blue and green arrows respectively in Fig. 2. It is obvious that working in high-energy stable region is desired, so the system should be designed to make the frequencies of ambient vibrations fall in this range.

Wide Bandwidth

The deflection of linear resonators drops dramatically when the system goes off-resonance, and a sharp peak that has a narrow bandwidth is formed. In contrast, it can be seen in Fig. 2 that for a nonlinear resonator, the deflection increases steadily in a wide frequency range before it jumps down to low level. By equating the stored energy due to nonlinear stiffness and an equivalent linear stiffness, we can find the

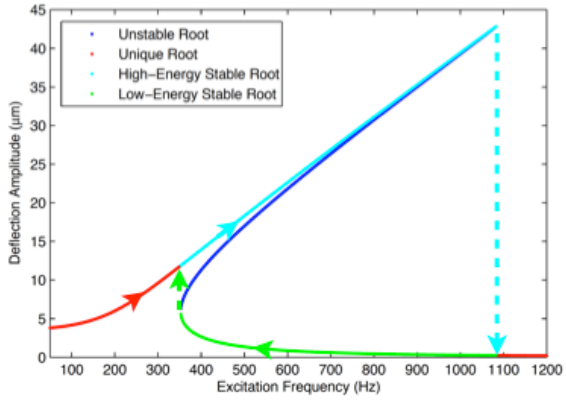

Figure 2. Simulation results of frequency response (deflection versus frequency).

equivalent stiffness to be $\frac{3}{4}k_N x^2$. Then, the equivalent natural frequency of the undamped nonlinear resonator can be estimated as,

$$\omega=\sqrt{\frac{k_L+0.75k_N x^2}{m}} \tag{4}$$

When the excitation frequency is lower than the jump-down frequency, the deflection tends to decrease from the peak value, but that decrease also lowers the resonant frequency of the nonlinear system, so that the system keeps working close to resonance. The nonlinear stiffness acts as a negative feedback which results in a much wider frequency range compared to a linear system.

Wide Power Bandwidth

In linear systems, the electrical impedance should match the mechanical impedance to achieve maximum power [6]. But for a nonlinear system, electrical damping can surpass the mechanical impedance to generate higher output power. By combining the mechanical elements in Fig. 1(c) except for nonlinear spring, a simplified electrical circuit with impedances is generated in Fig.1 (d). Z_M, Z_N, Z_E are mechanical impedance, impedance of nonlinear spring and electrical impedance respectively. It is obvious that when electrical impedance increases, the total impedance tends to increase, which will make the deflection drop, but the variable nonlinear impedance $\frac{0.75k_N x^2}{s}$ also tends to decrease because of the smaller x, and that tends to decrease the total impedance and increase the deflection. Consequently, this nonlinear impedance serves as a negative feedback and stabilizes the deflection when electrical damping changes. This effect can be clearly seen in Fig. 3(a) which compares the normalized deflections of a linear system and a nonlinear system with various total damping. Fig. 3(b) shows that for either fixed or varying electrical damping, the bandwidth of nonlinear system is much wider than that of linear systems.

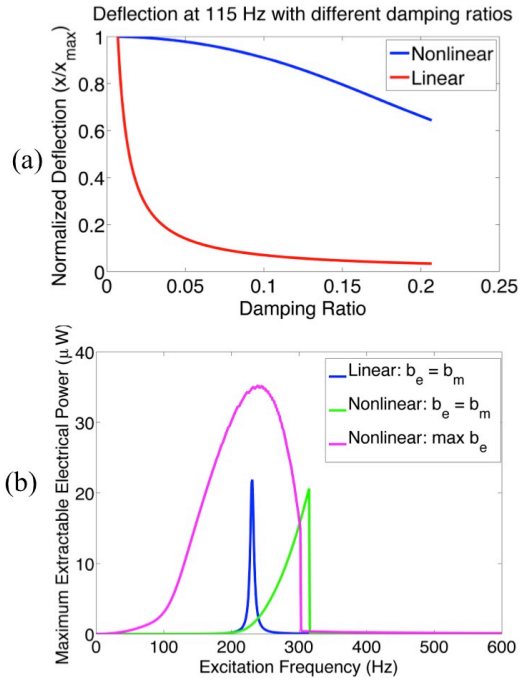

Figure 3. Comparison between linear and nonlinear systems behavior (simulation). (a) Deflection of linear and nonlinear systems versus damping ratio. (b) Maximum extractable electrical power comparison.

Since extractable electrical power is proportional to electrical damping, we can increase the output power by increasing electrical damping until it pushes the resonator into instability, resulting in jump-down to low energy state. A smart electronic interface such as adaptive SSHI will be ideal to implement this. Fig. 3(b) compares the maximum extractable power of linear and nonlinear systems.

EXPERIMENTS

Fabrication

Surface and bulk micro-machining processes were employed to implement the doubly-clamped beam based nonlinear energy harvester design. The fabricated device consists of four identical doubly-clamped beams which are connected to a single external proof mass (Fig. 4). The multi-layer structure of doubly-clamped beams consists of a structural layer (thermal oxide, low pressure chemical vapor deposition (LPCVD) silicon nitride, low temperature oxide (LTO)), a diffusion barrier layer (ZrO_2) which prevents electrical charge diffusing from piezoelectric layer, a thin film (0.27μm) of lead-zirconate-titanate (PZT) as the active layer to generate electricity under bending and stretching, and a top Ti/Al interdigitated electrodes extracting electrical charge generated in the PZT layer via d_{33} mode piezoelectric effect. Reactive ion etching (RIE) and deep RIE (DRIE) were used to pattern the structural layer. Less than 10MPa vertically

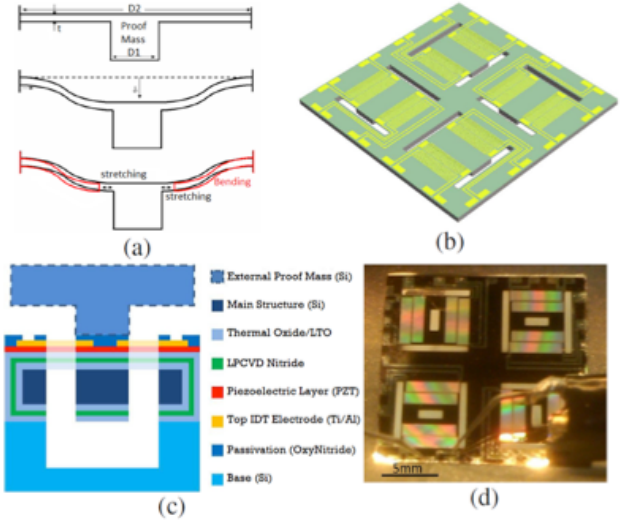

Figure 4. Nonlinear piezoelectric micro energy harvester (a) A doubly-clamped beam with large deflection. (b) 3D model of the energy harvester which consists of four doubly-clamped beams. (c) A schematic cross-sectional view of the harvester. (d) Optical image of the released device. [3]

symmetric residual stress is achieved to keep the working frequency low and to enhance the nonlinearity. The total thickness of the beam is ~5.5 μm. The final device is about the size of a US quarter coin. The schematic cross-sectional view of each layer is shown in Fig. 4(c).

Except the external proof mass, which has relatively large dimensions and was attached to the four doubly-clamped beams in the last step, the main structure of the energy harvester is monolithic. No additional assembly guarantees the feasibility of commercially deployable MEMS-scale products.

Electromechanical Test Results

The fabricated and packaged device was tested by using an electromagnetic shaker. Motion of the central proof mass and the base is measured remotely by a Doppler-effect laser vibrometer, and output voltage was measured and analyzed by Fast Fourier Transform (FFT) analyzer. The test results in Fig. 5(a) show up to 1.5V (peak-to-peak) open circuit output voltage. Based on the measured open-circuit voltage, the internal capacitance (8.5nF) and resistance (3.5MΩ), the generated power is shown in Fig. 5 (b) as curve 2 in comparison to the maximum theoretically extractable power (curve 1). The results show more than one order of magnitude improvements in bandwidth (>20% of the peak frequency) and two orders of magnitude improvements in power density (up to $2W/cm^3$ with an SSHI interface) in comparison to the devices previously reported [1, 2, 7, 8].

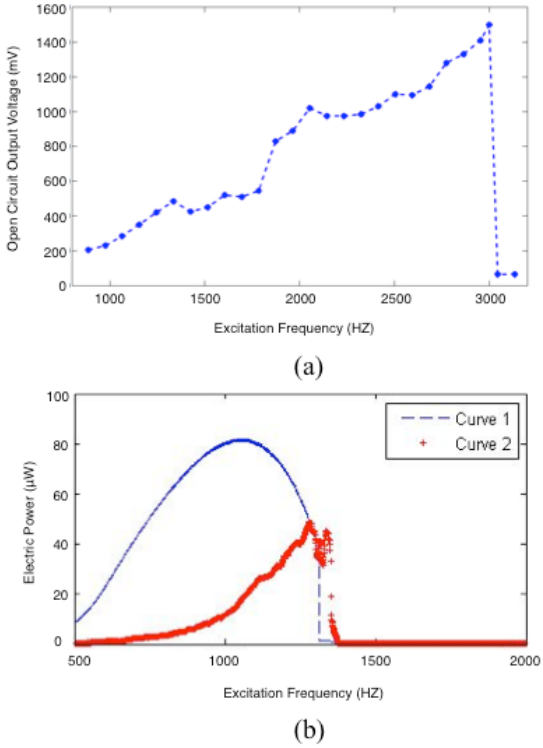

Figure 5. Electromechanical testing results. (a) Measured open-circuit voltage. (b) Curve 1 shows the theoretically-extractable power assuming ideal electric loading. Curve 2 depicts the generated power based on the measured open-circuit voltage.

DISCUSSION

The actual generated power in this case is smaller than the maximum extractable power, which can be easily scaled up by placing more (or thicker) layers of PZT and adjusting the electric load to exploit the high electrical damping capacity of the non-linear beam. Considering the volume of PZT ($4\times5mm\times4mm\times 265nm \approx 0.021mm^3$), the generated power density is 2W/cm^3. To better scavenge energy from ambient vibrations, which typically have low frequency spectra and low-g excitation, new features such as low working frequency (100~200 Hertz) and low excitation level (~0.5g) need to be integrated to our wide bandwidth energy harvester design. Analytical analysis shows that these improvements can be achieved by reducing the residual stress and the total thickness of the beam and by increasing the proof mass. Numerical simulations of the low-frequency, low-g design is shown in Fig. 6, which is under development.

CONCLUSION

We have demonstrated a new nonlinear design, which has much wider bandwidth and higher output power than the conventional linear resonant beam designs. The electromechanical test results have shown up to 1.5V open circuit voltage which can be interpreted to 2W/cm^3 power density based on an SSHI interface at 1.3 KHz. They also show at least one order of magnitude improvement in bandwidth (>20% of the peak frequency), which matches well the theoretical

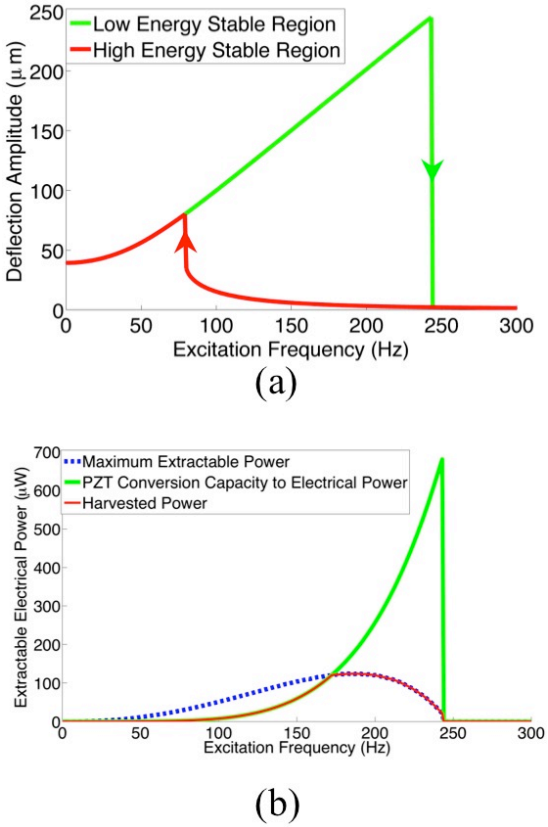

Figure 6. Simulations of a low-frequency, low-g (0.5g), wide-bandwidth energy harvester design. (a) Deflection versus frequency. The arrows denote the jumps. (b) Predicted extractable power of new design.

expectation. We anticipate that this wide bandwidth piezoelectric micro energy harvester will enable a wide range of self-powered devices.

REFERENCES

[1] Jeon Y.R., Sood R., Kim S.G., "Piezoelectric Micro Power Generator for Energy harvesting," *Sensors and Actuators A: Physical*, **122**, pp. 16-22, 2005.

[2] Hajati A., Kim S.G., "Wide-Bandwidth MEMS-Scale Piezoelectric Energy Harvester," *PowerMEMS*, Washington, DC, 2009, 269-272.

[3] Hajati A., Kim S.G., "Ultra-wide bandwidth piezoelectric energy harvesting," Applied Physics Letters, **99**, 083105, 2011.

[4] Senturia S.D., Microsystem Design, Springer, 2001.

[5] Nayfeh A. H., Nonlinear Oscillations, New York : Wiley, 1979.

[6] duToit N., Wardle B., Kim S.G., 2005 Integrated Ferroelectrics 71, 121–160.

[7] Beeby S.P., M. J. Tudor, N. M. White, Measurement Science and Technology **17**, 175-195, 2006.

[8] Hajati A., Bathurst S.P., Lee H., Kim S.G., "Design and fabrication of a nonlinear resonator for ultra wide-bandwidth energy harvesting applications," *Micro Electro Mechanical Systems (MEMS)* 2011, 1301-1304.